Nanocube Synthesis

Large-Scale Synthesis of Silver Nanocubes: The Role of HCl in Promoting Cube Perfection and Monodispersity**

*Sang Hyuk Im, Yun Tack Lee, Benjamin Wiley, and Younan Xia**

Shape control of metal nanoparticles has received considerable attention in recent years because of the strong correlation between the shape and the chemical, physical, electronic, optical, magnetic, and catalytic properties of a nanoparticle.[1] Silver and gold, in particular, have been intensively studied owing to their numerous applications that include surface plasmonics, surface-enhanced Raman scattering (SERS), as well as chemical and biological sensing.[2] A wealth of chemical methods have been developed for the synthesis of silver and gold nanostructures that have well-controlled shapes, including triangular plates,[3] cubes,[4] belts,[5] wires,[6] rods,[7] and branched multipods.[8] Most of these methods, however, still require improvement in terms of yield, purity, monodispersity, and scale of synthesis before they will find use in commercial applications. We and other groups have established the polyol process as a means to synthesize silver and gold nanoparticles with controllable shapes in relatively large quantities.[4–6] Furthermore, we discovered that single-crystal cubes and tetrahedrons of silver with truncated corners/edges could be prepared in high yields through the selective etching and dissolution of twinned seeds by chloride ions and oxygen (from air).[9] Herein, we report another highly effective mediator—hydrochloric acid—for the production of single-crystal nanocubes. The yield, perfection of the cube, and monodispersity of the sample are all greatly improved by employing HCl. More importantly, the robustness of this reaction even allows it to be carried out in a disposable vial submerged in an oil bath and heated on a hotplate. The dependence of morphology on the concentration of hydrochloric acid was also investigated, and the synthesis was successfully scaled up to produce silver nanocubes on the gram scale.

In a typical polyol synthesis, silver atoms are obtained by reducing $AgNO_3$ with ethylene glycol (EG) through reactions (1) and (2).[10]

$$2\,HOCH_2CH_2OH \rightarrow 2\,CH_3CHO + 2\,H_2O \quad (1)$$

$$2\,Ag^+ + 2\,CH_3CHO \rightarrow CH_3CHO{-}OHCCH_3 + 2\,Ag + 2\,H^+ \quad (2)$$

Once the concentration of silver atoms has reached the supersaturation value, they will start to nucleate and grow into nanoparticles. At the same time, nitric acid generated in situ activates a backward reaction that dissolves the solid silver that is initially formed [Eq. (3)].[11] Through the introduction of HCl, reaction (3) could be driven further to the right owing to the formation of more HNO_3 from HCl and $AgNO_3$.

$$4\,HNO_3 + 3\,Ag \rightarrow 3\,AgNO_3 + NO + 2\,H_2O \quad (3)$$

On the basis of these reactions and experimental observations, we can explain why and how perfect single-crystal silver nanocubes were formed in high yields. First, upon addition of silver nitrate and PVP (poly(vinyl pyrrolidone)) to the hot solution of EG, both twinned and single-crystal seeds of silver are formed through homogeneous nucleation, with the twinned particles being the most abundant morphology as a result of their relatively lower surface energies.[12] These initially formed nanoparticles are dissolved owing to the relatively high concentration of HNO_3 present in the early stages of the reaction. As the reaction continues, HNO_3 is gradually consumed and a second round of nucleation occurs. At very small sizes, it is expected that the crystal structure of these nuclei fluctuates, as has been observed in several TEM

[*] Dr. S. H. Im, Y. T. Lee, Prof. Y. Xia
Department of Chemistry
University of Washington
Seattle, WA 98195 (USA)
Fax: (+1) 206-685-8665
E-mail: xia@chem.washington.edu
B. Wiley
Department of Chemical Engineering
University of Washington
Seattle, WA 98195 (USA)

[**] This work was supported in part by ONR (N-00014-01-1-0976) and a fellowship from the David and Lucile Packard Foundation. Y.X. is an Alfred P. Sloan Research Fellow and a Camille Dreyfus Teacher Scholar. Both S.H.I. and Y.T.L. have been partially supported by the Postdoctoral Fellowship Program of the Korean Science and Engineering Foundation (KOSEF). B.W. thanks the Center for Nanotechnology at the University of Washington for an IGERT Fellowship Award supported by the NSF (DGE-9987620).

Supporting information for this article is available on the WWW under http://www.angewandte.org or from the author.

  DOI: 10.1002/ange.200462208

studies.[13] When the nanoparticles grow in dimension, they will be locked into either a single-crystalline or twinned morphology. While the twinned particles have a lower overall surface energy, this comes at the expense of significant lattice distortion and surface defects. Thus, twinned particles are expected to exhibit a stronger reactivity and susceptibility towards etching. As no lattice distortion is required to form a single crystal, these seeds should be relatively more stable in this environment and can continue to grow. Consequently, through the selective etching of twinned seeds by HNO_3, high yields of single-crystal nanocubes result (see Supporting Information for a schematic of this mechanism).

While selective etching is the dominant mechanism for producing nanocubes, there are additional elements that contribute to its success. In the present study, both the proton and the chloride ion of HCl play a significant role. As well as its function in increasing the concentration of HNO_3, the proton can greatly reduce the net reaction rate according to Le Chatelier's principle. At the same time, chloride ions likely adsorb onto the surfaces of silver seeds and thereby prevent agglomeration through electrostatic stabilization.[14] We also lowered the reaction temperature from 160 to 140 °C to further slow down the net reaction rate in an effort to increase the efficiency of selective etching by nitric acid. This combination of factors allies to promote the production of silver nanocubes with high yields and monodispersed sizes.

The primary stages of the reaction can be recognized by their distinctive colors. As illustrated in Figure 1 a, the solution turned milky white after the injection of the solutions of $AgNO_3$ and PVP. This color suggests the presence of AgCl precipitate caused by the relatively high concentration of chloride ions in the reaction mixture (0.25 mM). Figure 1 e shows a TEM image of a sample taken from the suspension at this stage. The chemical composition of these particles was AgCl, as confirmed by both X-ray diffraction (XRD) and energy dispersive X-ray (EDX) analyses. At $t = 45$ min, the solution turned light yellow in color (Figure 1 b) which indicates that the AgCl particles had dissolved and only Ag nanoparticles remained in the reaction mixture. As shown by TEM (Figure 1 f), Ag nanoparticles of two different sizes (diameter, $d \approx 20$ and ≈ 5 nm) coexist in the solution at this time. The light yellow color gradually faded, and the solution appeared transparent and colorless at around $t = 105$ min (Figure 1 c) which suggests the complete dissolution of all large Ag nanoparticles. This picture is also consistent with TEM observations (Figure 1 g) in which only very few Ag nanoparticles of very small size ($d \approx 6$ nm) could be found. This transparent state lasted for approximately one hour, after which time the solution acquired a reddish tint whose intensity increased over a period of several hours. By $t = 15$ h, the solution had become red (as shown in Figure 1 d), implying the formation of small Ag nanocubes. A typical TEM image (Figure 1 h) of these Ag nanocubes shows that they were perfect in shape and approximately 30 nm in edge length. These Ag nanocubes could further grow into cubes of larger sizes if the reaction was allowed to continue. Finally, the solution became ocher in color at approximately $t = 26$ h. The Ag nanocubes contained in this solution were also perfect in shape with their edge length increased to around 130 nm.

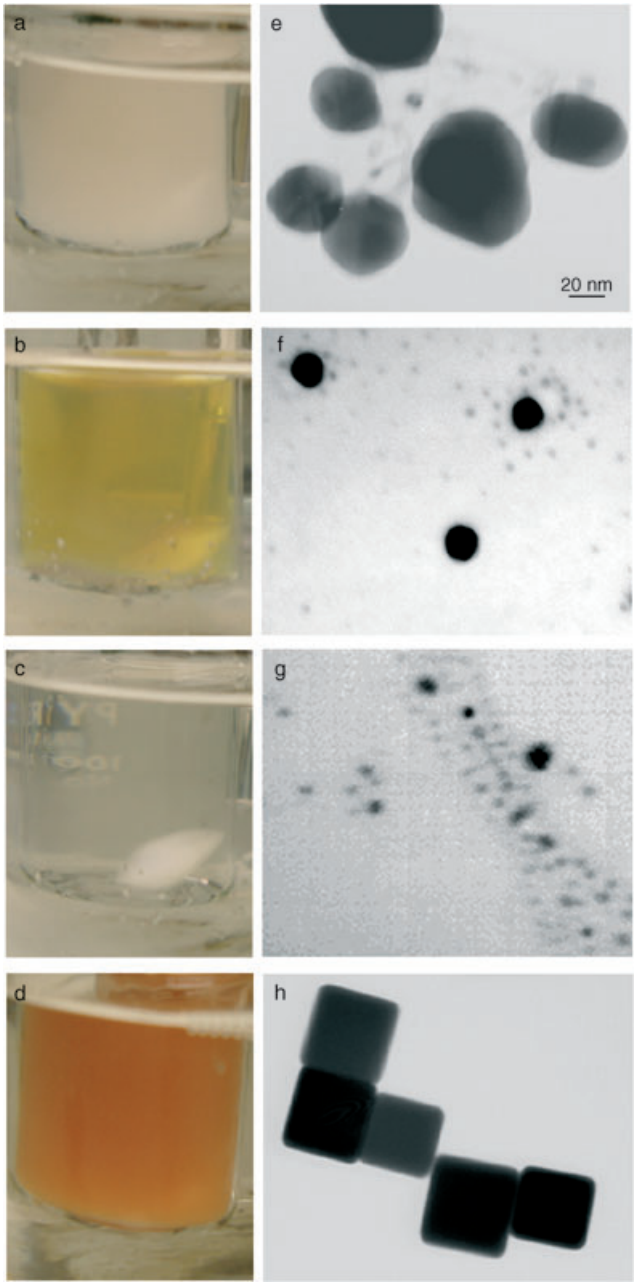

Figure 1. Morphological revolution with reaction time. a)–d) Photographs of the reaction solution at $t = 4$, 46, and 103 min, and 15 h, respectively. e)–h) TEM images of silver nanoparticles contained in the corresponding reaction solution shown on the left (a–d).

This observation implies that it will be possible to control the size and therefore the optical properties of Ag nanocubes simply by varying the reaction time. Figure 2 demonstrates the size-dependent absorption spectra of the cubes. The number of peaks and relative positions are consistent with theoretical calculations.[15]

The dependence of morphology on the concentration of HCl was also examined. Figure 3 a shows the SEM image of a product obtained at $t = 25$ h when the concentration of HCl was 0.125 mM in the final mixture. This sample contained a mixture of polydisperse silver nanocubes, tetrahedrons, and

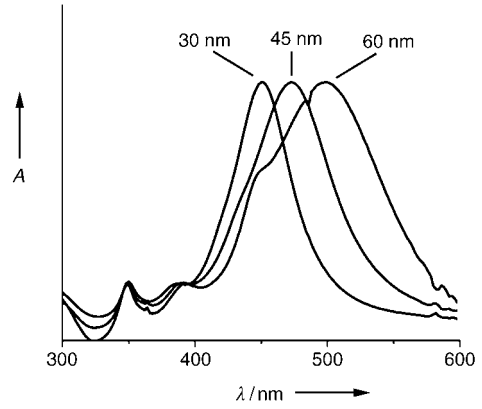

Figure 2. UV/Vis absorption spectra of aqueous solutions that contain silver nanocubes with different edge lengths (30, 45, and 60 nm).

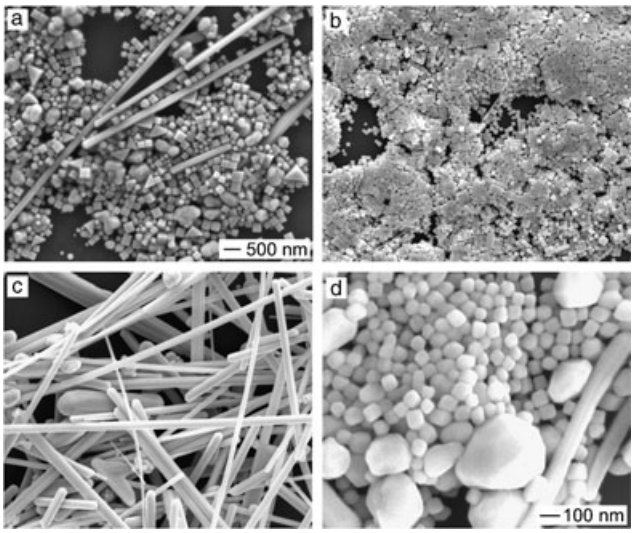

Figure 3. SEM images of silver nanoparticles synthesized at different concentrations of HCl (scale bar: 500 nm): a) 0.125, b) 0.25, and c) 0.375 mM, respectively. The reaction solution contained $AgNO_3$ (23.5 mM) and PVP (36.7 mM, calculated in terms of the repeating unit) and was heated in an oil bath held at 140 °C. d) Silver nanoparticles obtained under the same conditions except that HNO_3 (0.25 mM) was used instead of HCl (0.25 mM).

nanowires. It is believed that the wires and irregular particles form as a result of the incomplete etching of twinned seeds by the lower concentration of HNO_3. Figure 3b shows an SEM image of the final product obtained at $t = 26$ h when the concentration of HCl was increased to 0.25 mM (namely, the synthesis described in Figure 1). The solution contained only monodisperse silver nanocubes of about 130 nm in edge length. As the concentration of HCl was further increased to 0.375 mM, a different morphology was observed (Figure 3c). This product, obtained at $t = 22$ h, was characterized by a mixture of relatively thick wires and irregular particles. The mechanism behind this morphological variant is yet to be understood. In this case, it was found that the reaction mixture did not become transparent which indicates that the twinned seeds were not dissolved to cut short their growth into nanowires and irregular particles. It is assumed that chloride ions could slow down the etching of twinned seeds by selectively blocking the twin sites through surface adsorption. Alternatively, it is possible that an increase in the concentration of HCl may result in the formation of more AgCl precipitate at the initial stage of the synthesis and that some of these AgCl colloids may survive and serve as seeds for the subsequent growth of twinned particles. On the basis of the results of these experiments, it is concluded that 0.25 mM represents an ideal concentration of HCl for the synthesis of silver nanocubes.

To separate the roles played by the proton and chloride, we also replaced HCl (0.25 mM) with HNO_3 (0.25 mM). The NO_3^- ions from HNO_3 should have a negligible effect on the synthesis because the concentration of HNO_3 was extremely low as compared to the concentration of $AgNO_3$. Figure 3d shows a typical SEM image of the product at $t = 30$ h that comprised a mixture of small silver nanocubes (edge length ≈ 40 nm) and some irregular particles. This observation implies that HNO_3 alone is able to induce the etching and dissolution of twinned seeds and thus channel the product into single-crystal nanocubes. However, owing to the absence of Cl^- ions in the solution, the single-crystal seeds could not be stabilized and therefore might agglomerate into larger, irregularly shaped particles. It is also expected that a combination of Cl^- ions and O_2 will facilitate the etching and dissolution of twinned seeds to further decrease the percentage of twinned particles in the final product.

It is an important issue to scale up the synthesis from the viewpoint of commercial usage. To this end, we increased the volumes of all solutions by a factor of five. In this case, the synthesis followed the same pattern of color changes which suggests that the nucleation and growth mechanisms did not change as the reaction volume was increased. Figure 4a shows

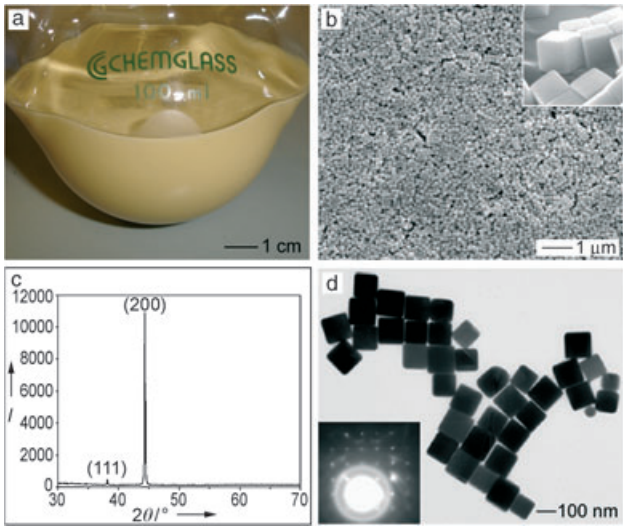

Figure 4. a) Photograph of the reaction mixture in a scale-up (×5) synthesis. b) Typical SEM images of the as-synthesized silver nanocubes. The inset shows a magnified SEM image that illustrates the sharp corners and edges of these nanocubes. c) An XRD pattern of the same batch of silver nanocubes. d) TEM image of the silver nanocubes. The inset shows an electron diffraction pattern recorded by directing the electron beam perpendicular to the (100) facet of a silver nanocube.

a photograph of the final product, which displayed an ocher color similar to that seen for the smaller reaction volume. Figure 4b shows a typical SEM image of this sample and indicates that all particles were cubic in shape with an average edge length of 125 nm. The inset shows a tilted SEM image at higher magnification that clearly displays the sharp corners and edges of these nanocubes. Figure 4c shows an XRD pattern recorded from the same batch of silver nanocubes. The abnormal intensity of the (200) peak suggests that the sample exclusively comprises nanocubes that were preferentially oriented with their (100) planes parallel to the supporting substrate. Figure 4d shows a typical TEM image of the silver nanocubes. Again, it is clear that these silver nanocubes are single crystals with sharp corners and edges. The inset shows an electron diffraction pattern recorded by directing the electron beam perpendicular to the (100) facet of an individual nanocube and confirms that the particles are single crystals.

In summary, monodispersed nanocubes of silver have been synthesized in large quantities by introducing a small amount of hydrochloric acid to the conventional polyol synthesis. From the color changes involved and electron microscopy studies, it is believed that hydrochloric acid plays an important role in selectively etching and dissolving twinned silver nanoparticles. In contrast to our previous work based on the mediation of NaCl, the current process is more robust as it involves two different types of etchants: HNO_3 and Cl^-/O_2. Furthermore, the presence of protons greatly slows down the reduction reaction and thereby facilitates the formation of single-crystal seeds. Under the optimized conditions, we have been able to scale up the synthesis to 0.25 grams (or 1.2×10^{21} 130-nm-wide cubes).

Experimental Section

In a typical synthesis, ethylene glycol (EG; 5 mL, J. T. Baker, 9300-01) was placed in a 20-mL vial, capped, and heated with stirring in an oil bath at 140 °C for 1 h. HCl (1 mL of a 3 mM solution in EG) was then quickly added, and the vial was recapped. After 10 min, $AgNO_3$ (3 mL of a 94 mM solution in EG; Aldrich, 209139–100G) and poly(vinyl pyrrolidone) (PVP; 3 mL of a solution in EG (147 mM in terms of the repeating unit); $M_r \approx 55000$, Aldrich, 856568-100G) were simultaneously added with a two-channel syringe pump (KDS-200, Stoelting, Wood Dale, IL) at a rate of 45 mL per hour to the stirring solution. The vial was then capped and heated at 140 °C. Upon injection of the solution of $AgNO_3$, the reaction mixture went through a series of color changes that included milky white, light yellow, transparent, red, and ocher. To separate the roles of the proton and chloride, we performed a synthesis under the same conditions except for the replacement of HCl by HNO_3. For the scale-up synthesis, the vial was replaced with a 100-mL flask, and the volumes of all solutions were increased by a factor of five.

All samples for morphology and structure analysis were washed with acetone and then with water to remove excess EG and PVP. SEM images were taken using a field emission scanning electron microscope (FEI, Sirion XL) operated at an accelerating voltage of 10–20 kV. The transmission electron microscopy (TEM) images and diffraction patterns were obtained using a JEOL microscope (1200EX II) operating at 80 kV. X-ray diffraction (XRD) studies were performed on a Philips 1820 diffractometer with a scan rate of 0.2 degrees per minute in the range 20–90°. UV/Vis absorption spectra were taken at room temperature on a Hewlett Packard 8452 spectrometer (Palo Alto, CA) using a quartz cuvette with an optical path of 1 cm.

Received: October 5, 2004
Published online: February 28, 2005

Keywords: aggregation · crystal growth · nanostructures · polyol synthesis · silver

[1] a) Y. Xia, P. Yang, Y. Sun, Y. Wu, B. Gate, Y. Yin, F. Kim, H. Yan, *Adv. Mater.* **2003**, *15*, 353; b) Y. Wu, B. Messer, P. Yang, *Adv. Mater.* **2001**, *13*, 1487; c) N. I. Kovtyukhova, T. E. Mallouk, *Chem. Eur. J.* **2002**, *8*, 4354; d) C. Salzemann, I. Lisiecki, A. Brioude, J. Urban, M.-P. Pileni, *J. Phys. Chem. B* **2004**, *108*, 13243; e) N. R. Jana, L. Gearheart, S. O. Obare, C. J. Murphy, *Langmuir* **2002**, *18*, 922; f) A. T. Ngo, M. P. Pileni, *Colloids Surf. A* **2003**, *228*, 107; g) V. F. Puntes, K. M. Krishnan, A. P. Alivisatos, *Science* **2001**, *291*, 2115; h) Z. L. Wang, T. S. Ahmad, M. A. El-Sayed, *Surf. Sci.* **1997**, *380*, 302.

[2] a) D. Roy, J. Fendler, *Adv. Mater.* **2004**, *16*, 479; b) J. R. Krenn, *Nat. Mater.* **2003**, *2*, 210; c) K. Kneipp, Y. Wang, H. Kneipp, L. T. Perelman, I. Itzkan, R. R. Dasari, M. S. Feld, *Phys. Rev. Lett.* **1997**, *78*, 1667; d) J. P. Kottmann, O. J. F. Martin, D. R. Smith, S. Schultz, *Phys. Rev. B* **2001**, *64*, 235402; e) A. J. Haes, R. P. Van Duyne, *J. Am. Chem. Soc.* **2002**, *124*, 10596; f) B. D. Moore, L. Stevenson, A. Watt, S. Flitsch, N. H. Turner, C. Cassidy, D. Graham, *Nat. Biotechnol.* **2004**, *22*, 1133; g) Y. Cao, R. Jin, C. Mirkin, *Science* **2002**, *297*, 1536.

[3] a) R. Jin, Y. Cao, C. A. Mirkin, K. L. Kelly, G. G. Schatz, J. G. Zheng, *Science* **2001**, *294*, 1901.

[4] a) Y. Sun, Y. Xia, *Science* **2002**, *298*, 2176; b) R. Jin, S. Egusa, N. F. Scherer, *J. Am. Chem. Soc.* **2004**, *126*, 9900; c) T. K. Sau, C. J. Murphy, *J. Am. Chem. Soc.* **2004**, *126*, 8648; d) F. Kim, S. Connor, H. Song, T. Kuykendall, P. Yang, *Angew. Chem.* **2004**, *43*, 3759; *Angew. Chem. Int. Ed.* **2004**, *43*, 3673.

[5] Y. Sun, B. Mayers, Y. Xia, *Nano. Lett.* **2003**, *5*, 675.

[6] a) Y. Sun, B. Mayers, T. Herricks, Y. Xia, *Nano Lett.* **2003**, *3*, 955; b) Y. Sun, Y. Yin, B. Mayers, T. Herricks, Y. Xia, *Chem. Mater.* **2002**, *14*, 4736; c) Y. Sun, B. Mayers, Y. Xia, *Adv. Mater.* **2003**, *15*, 641.

[7] a) N. R. Jana, L. Gearheart, C. J. Murphy, *J. Phys. Chem. B* **2001**, *105*, 4065; b) C. J. Murphy, N. R. Jana, *Adv. Mater.* **2002**, *14*, 80; c) F. Kim, J. H. Song, P. Yang, *J. Am. Chem. Soc.* **2002**, *124*, 14316.

[8] a) E. Hao, R. C. Bailey, G. C. Schartz, J. T. Hupp, S. Li, *Nano Lett.* **2004**, *4*, 327; b) S. Chen, Z. L. Wang, J. Ballato, S. H. Foulger, D. L. Carroll, *J. Am. Chem. Soc.* **2003**, *125*, 16186.

[9] B. Wiley, T. Herricks, Y. Sun, Y. Xia, *Nano Lett.* **2004**, *4*, 1733.

[10] a) C. Özmetin, M. Çopur, A. Yartasi, M. M. Kocakerim, *Chem. Eng. Technol.* **2003**, *23*, 707; b) B. Blin, F. Fievet, D. Beaupère, M. Figlarz, *Nouv. J. Chim.* **1989**, *13*, 67.

[11] F. Fievet, J. P. Lagier, M. Figlarz, *MRS Bull.* **1989**, *14*, 29.

[12] Z. L. Wang, *J. Phys. Chem. B* **2000**, *104*, 1153; b) C. Cleveland, U. Landman, *J. Chem. Phys.* **1991**, *94*, 7376; c) P. M. Ajayan, L. D. Marks, *Phys. Rev. Lett.* **1988**, *60*, 585.

[13] a) S. Iijima, T. Ichihashi, *Phys. Rev. Lett.* **1986**, *56*, 616; b) D. J. Smith, A. K. Petford Long, L. R. Wallenberg, J. O. Bovin, *Science* **1986**, *233*, 872; c) N. Doraiswamy, L. Marks, *Surf. Sci.* **1996**, *348*, L67.

[14] a) C. A. Mirkin, *Inorg. Chem.* **2000**, *39*, 2258; b) S. Lin, Y. Tsai, C. Chen, C. Lin, C. Chen, *J. Phys. Chem. B* **2004**, *108*, 2134.

[15] I. O. Sosa, C. Noguez, R. G. Barrera, *J. Phys. Chem. B 107*, 6269.

